

# Improved precision in measurements of acoustic impedance spectra using resonance-free calibration loads and controlled error distribution

Paul Dickens,<sup>a)</sup> John Smith, and Joe Wolfe

*School of Physics, The University of New South Wales, Sydney 2052, Australia*

(Received 12 August 2006; revised 4 December 2006; accepted 27 December 2006)

Resonances and/or singularities during measurement and calibration often limit the precision of acoustic impedance spectra. This paper reviews and compares several established techniques, and describes a technique that incorporates three features that considerably improve precision. The first feature is to minimize problems due to resonances by calibrating the instrument using up to three different acoustic reference impedances that do not themselves exhibit resonances. The second involves using multiple pressure transducers to reduce the effects of measurement singularities. The third involves iteratively tailoring the spectrum of the stimulus signal to control the distribution of errors across the particular measured impedance spectrum. Examples are given of the performance of the technique on simple cylindrical waveguides. © 2007 Acoustical Society of America.

[DOI: 10.1121/1.2434764]

PACS number(s): 43.58.Bh, 43.75.Pq [AJZ]

Pages: 1471–1481

## I. INTRODUCTION

The input impedance of any one-dimensional waveguide is defined as the complex ratio of pressure to volume flow at the input. This quantity is used to describe the linear acoustics of automotive mufflers, air-conditioning ducts, and the passive elements of wind instruments and the vocal tract. For a musical instrument, the input impedance usefully displays important characteristics of the instrument in the absence of a player, and indicates how the instrument will respond when excited at any frequency. In this case, high resolution in magnitude and frequency are particularly important. If pressure and volume flow are measured at different points in a system, their ratio gives a transfer impedance, which is particularly useful in characterizing multiport systems.

In this paper, we review the various approaches to measuring acoustic impedance and calibrating impedance heads and propose a general calibration technique for heads with multiple transducers. We consider the effect of transducer errors on impedance measurements and present a technique for distributing any measurement errors over the frequency range. To demonstrate the technique we use an impedance head with three microphones to measure the input impedance of simple cylindrical waveguides. The effects of calibration and optimization on these measurements are presented and discussed.

## II. REVIEW OF MEASUREMENT TECHNIQUES

Many techniques for measuring acoustic impedance have been devised. The major techniques are reviewed by Benade and Ibbi<sup>1</sup> and Dalmont.<sup>2</sup> Any two transducers with responses that are linear functions of pressure and flow may be used to construct an impedance head; hence many designs are possible. In Table I, several common techniques are il-

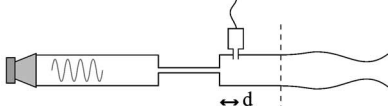
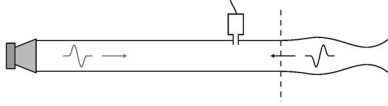
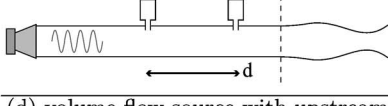
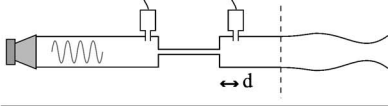
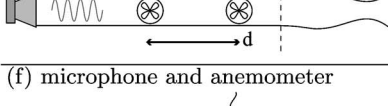
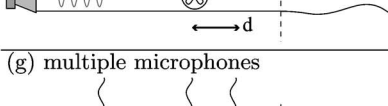
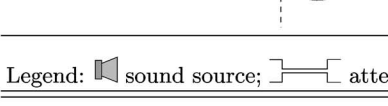
lustrated, along with conditions for singularities. At a singularity, the system of equations governing an impedance head becomes degenerate, and the impedance cannot be determined (see Sec. V E).

In methods (a) and (b) (Table I), a single pressure transducer (microphone) is used. In the volume flow source method (a) the input impedance is proportional to the ratio of the pressure measured with the unknown load to that with a reference load using the same stimulus. An attenuator ensures a source of volume flow, provided the impedance of the attenuator is much greater than that of the unknown load. (The effect of a finite source impedance can be reduced, to first order, by subtracting the attenuator admittance from the measured admittance.) In (b), a method known as pulse reflectometry, a pressure pulse is recorded as it travels toward the load, and again as it returns, yielding the impulse response function. This is mainly used for area reconstruction of musical wind instruments<sup>3</sup> and the airway,<sup>4</sup> however the acoustic impedance can be obtained from the impulse response function after a Fourier transform.

In methods (c) to (e) two similar transducers are used simultaneously. In methods (c) and (e), neither transducer measures pressure or flow at the input to the load alone; these are obtained by computations involving the transfer functions of the duct and the transducer properties. If a linear attenuator is present between the two microphones, as in method (d), the pressure difference between the two microphones is proportional to the flow. Alternatively, a signal approximately proportional to flow may be obtained by measuring the pressure in a fixed cavity at the back of the driver.<sup>5</sup> Impedance heads have also been devised using a pressure transducer and a flow transducer (f), yielding the impedance with a minimum of computation (provided both transducers are close enough to the reference plane). Because of the difficulties in measuring flow precisely, these have limited dynamic range and signal-to-noise ratio.

<sup>a)</sup>Electronic mail: pdickens@phys.unsw.edu.au

TABLE I. Several of the more common impedance heads, with conditions for singularities, selected references, and notes. In the expressions for singularities,  $k$  is the wave number and  $n=1,2,3,\dots$ . The reference plane is indicated by a vertical dashed line.

Impedance Head	Singularities	Refs.	Notes
(a) volume flow source 	$kd = (2n - 1)\frac{\pi}{2}$	1, 5-7	<ul style="list-style-type: none"> <li>• computationally simple</li> <li>• requires calibration of the source</li> <li>• prone to errors at high <math> Z </math></li> </ul>
(b) pulse reflectometer 	$f$ -range limited by 3, 4 pulse width		<ul style="list-style-type: none"> <li>• uses same microphone for incident and reflected wave; calibration unnecessary</li> <li>• accuracy limited by length of measurement duct</li> </ul>
(c) two microphones 	$kd = (n - 1)\pi$	8-15	<ul style="list-style-type: none"> <li>• fewer simplifying assumptions required</li> <li>• computationally intensive</li> </ul>
(d) volume flow source with upstream microphone 	$kd = (2n - 1)\frac{\pi}{2}$	16-18	<ul style="list-style-type: none"> <li>• signal from upstream microphone proportional to flow (for an attenuator with high impedance compared to the unknown load)</li> </ul>
(e) two anemometers 	$kd = (n - 1)\pi$	19	<ul style="list-style-type: none"> <li>• computationally similar to (c)</li> <li>• several particle velocity sensors can be made simply with similar characteristics</li> </ul>
(f) microphone and anemometer 	$kd = (2n - 1)\frac{\pi}{2}$	20-22	<ul style="list-style-type: none"> <li>• direct measurement of both pressure and flow</li> <li>• correction required to obtain volume flow from particle velocity</li> </ul>
(g) multiple microphones 	vary with microphone spacings	23	<ul style="list-style-type: none"> <li>• wide frequency range</li> <li>• increased precision</li> </ul>
Legend:  sound source;  attenuator;  microphone;  flow sensor			

The signal-to-noise ratio and frequency range may both be increased if an array of more than two transducers is used. Such a system with three microphones is shown in method (g).

### III. THEORY OF ACOUSTIC IMPEDANCE MEASUREMENTS

A general impedance head is shown in Fig. 1. Some source of acoustic energy (shown here as a loudspeaker) excites the air inside a conduit (usually cylindrical) and transducers along the conduit measure some signal proportional to pressure and flow. The impedance is measured at some reference plane, to which load impedances may be attached.

The air inside the conduit is excited at frequencies below the cut-on frequency of the first higher mode, which for a cylindrical duct of radius  $a$  occurs at  $f=1.84c/2\pi a$ , where  $c$  is the speed of sound.<sup>24</sup> Therefore, all modes except the

plane wave mode are nonpropagating. If higher modes are excited near the transducers and the reference plane, the measured impedance will be something other than the plane-wave impedance. The effect of discontinuities at the transducers may be removed by calibration. If a discontinuity exists at the reference plane, nonpropagating modes are excited, introducing errors into the measured plane wave im-

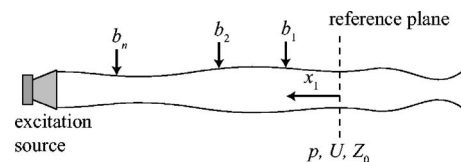


FIG. 1. A generalized impedance head. Impedance is measured at the *reference plane*, where the pressure, volume flow, and characteristic impedance are given by  $p$ ,  $U$ , and  $Z_0$ , respectively. The volume flow is positive flowing *into* the unknown load.  $n$  sensors record the signals  $b_1, b_2, \dots, b_n$  and are at positions  $x_1, x_2, \dots, x_n$ , measured from the reference plane.

pedance. Hence it is preferable that the object under study couple smoothly to the measurement conduit—otherwise multimodal theory can be used to calculate a correction (see Sec. V C).

It should be noted that in some impedance heads, the source and any transducers are located at or very near the reference plane; the sketch in Fig. 1 should be considered a general case only. However, it is often desirable to separate the source from the transducers, to ensure that the acoustic waves are planar at the transducers, subject to the constraints discussed in Sec. V.

For an impedance head with  $n$  transducers ( $n \geq 2$ ), the pressure  $p$  and flow  $U$  at the reference plane are given by the vector  $\mathbf{x}$  in a matrix equation of the form  $\mathbf{Ax}=\mathbf{b}$ :

$$\begin{bmatrix} A_{11} & A_{12} \\ A_{21} & A_{22} \\ \vdots & \vdots \\ A_{n1} & A_{n2} \end{bmatrix} \begin{bmatrix} p \\ Z_0 U \end{bmatrix} = \begin{bmatrix} b_1 \\ b_2 \\ \vdots \\ b_n \end{bmatrix}, \quad (1)$$

where  $\mathbf{b}$  is a vector of transducer signals and the elements of each matrix are, in general, functions of frequency. In order for the matrix  $\mathbf{A}$  to be dimensionless, any quantities with units of volume flow are parametrized by the characteristic impedance of the head at the input,  $Z_0$ . Thus  $\mathbf{x}$  and  $\mathbf{b}$  both have units of pressure.

For ideal transducers positioned a known distance from the reference plane and mounted in a cylindrical duct, the elements of  $\mathbf{A}$  are given by the transfer matrix for a straight tube. The signal from an ideal pressure transducer with unity gain at position  $x$  is given by

$$b_{\text{pressure}}(x) = \cosh(ikx)p + \sinh(ikx)Z_0U \quad (2)$$

and the signal [ $b_{\text{flow}}(x) \equiv Z_0U(x)$ ] from an ideal flow transducer (again at  $x$  and with unity gain) is given by

$$b_{\text{flow}}(x) = \sinh(ikx)p + \cosh(ikx)Z_0U, \quad (3)$$

where  $k = \omega/v - i\alpha$  where  $i = \sqrt{-1}$  and  $v$  and  $\alpha$  (the phase velocity and attenuation coefficient) are calculated taking into account viscothermal loss (see, e.g., Fletcher and Rossing<sup>24</sup>). From these, the matrix  $\mathbf{A}$  may be built up for any combination of transducers.

Once  $\mathbf{A}$  is determined, the pressure and flow (and hence the impedance) for a given measurement  $\mathbf{b}$  are obtained by solving Eq. (1). The equation is solved in the normal algebraic sense for  $n=2$ . For  $n > 2$ , there are more equations than are algebraically necessary to determine the pressure and flow. In this case Eq. (1) is solved using a least-squares method.

Determining  $\mathbf{A}$  from theory does not take into account perturbation of the wave by the transducers or nonidentical transducer responses and also requires an accurate knowledge of the complex wave number  $k$ , which depends significantly on temperature, humidity, and surface roughness. For these reasons, one or more calibrations are often used to determine  $\mathbf{A}$ .

## IV. CALIBRATION OF IMPEDANCE HEADS

### A. Review of calibration techniques

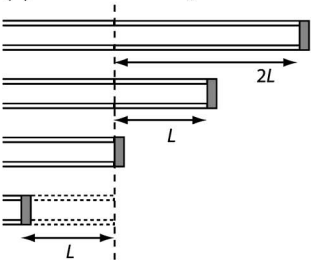
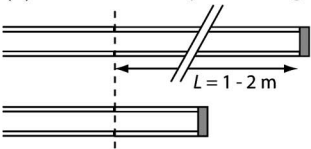
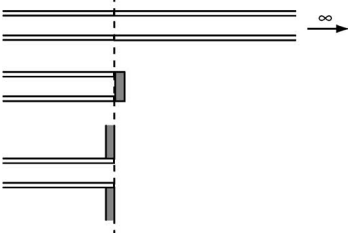
An impedance head can be constructed with two or more transducers that respond linearly to changes in pressure and flow. This includes, for example, microphones with non-negligible compliance and transducers with frequency-dependent gain. These are mounted in a waveguide which need not be cylindrical, and the exact positions of each transducer need not be known. Such a system may be calibrated fully by measuring its response to three test loads of known impedance. For a head with two microphones, three complex parameters must be determined, e.g., the gain ratio of the microphones, the admittance of the microphone closest to the unknown load, and the complex wave number for propagation within the waveguide, although other physical quantities such as the distance to each microphone may be used as parameters. Hence the ratios of microphone signals from three known loads are required to fully calibrate the system. If there are more than two microphones, the calibration parameters are overdetermined with three calibration loads, but two is not enough. If some assumptions can be made about the impedance head, then the number of calibrations required is reduced.

Gibiat and Laloë<sup>13</sup> describe a complete calibration routine for the two-microphone method [calibration loads (a) in Table II]. They use two stopped pipes of diameter equal to that of the measurement head, and a quasi-infinite impedance (a solid stop at the reference plane) to determine three calibration functions. The lengths of the two stopped pipes must be chosen carefully so that a range of impedances is encountered at each frequency. For example, if a calibration pipe has a resonance at a frequency of interest, its input impedance at that frequency will be very similar to that of the solid stop, and the calibration functions will have large errors at that frequency. For measurements of acoustic impedance over a wide frequency range, several microphone spacings are needed, each with its own set of calibration loads.

The two-microphone-three-calibration (TMTTC) technique described earlier<sup>13</sup> depends on accurate knowledge of the impedances of the test pipes; this in turn requires accurate knowledge of the complex wave number, a quantity that is strongly dependent on measurement conditions and the surface characteristics of the test pipes. Calibration using resonant pipes explicitly depends on a theory for wall losses. Further, the temperature and humidity must be accurately determined, and the test pipes must be very accurately machined. If an extra calibration is available, then the complex wave number need not be known; this is the approach of van Walstijn *et al.*,<sup>15</sup> who employ the three calibrations of Gibiat and Laloë plus a “negative length” tube, realized by defining the reference plane some distance from the first microphone.

Dalmont<sup>25</sup> presents a calibration technique for impedance heads with a volume flow source, which may also be extended to the two-microphone case<sup>2</sup> [calibration loads (b) in Table II]. The method is based on resonance analysis of a long closed tube. The impedance of the tube is measured using the uncalibrated head and the attenuation coefficient and wave number are derived from the measurement. When

TABLE II. Several techniques for calibration of impedance heads, with selected references and notes.

Calibration Loads	Refs.	Notes
(a) TMTTC technique 	13, 15	<ul style="list-style-type: none"> <li>• ‘complete’ calibration with three known loads</li> <li>• several sets of calibration loads needed to cover wide <math>f</math>-range</li> <li>• complex wavenumber need not be known if a fourth ‘negative length’ load is used</li> </ul>
(b) resonance analysis of long tube 	7, 25	<ul style="list-style-type: none"> <li>• after initial measurement of <math>Z</math> for long tube, calibration parameters determined from oscillations in <math>\alpha</math> and <math>k</math></li> <li>• complex wavenumber need not be known if an extra short tube is used</li> <li>• data obtained only at resonances and antiresonances of long tube—low frequency limit determined by length of tube</li> </ul>
(c) semi-infinite pipe 	6	<ul style="list-style-type: none"> <li>• almost purely resistive load—impedance insensitive to complex wavenumber</li> <li>• used for calibration of volume flow sources</li> </ul>
(d) resonance-free loads 		<ul style="list-style-type: none"> <li>• complete calibration as in (a)</li> <li>• valid for all frequencies, due to lack of resonances</li> <li>• the flange calibration may be omitted if a model of the impedance head is available</li> </ul>

plotted against frequency these will show periodic oscillations with amplitude proportional to any errors in calibration. The three calibration constants are estimated from these oscillations, and the procedure is repeated until the oscillations are tolerably small. The main advantage of this procedure is that it does not depend on exact knowledge of the complex wave number. The main disadvantage is that it only yields calibration data at each resonance frequency of the calibration tube. These may be interpolated, but the lowest frequency that can be measured is limited by the length of the calibration tube (and is around 80 Hz for a 2 m tube—and higher for shorter tubes).

### B. General calibration technique using up to three resonant-free loads

Here, we calibrate a three-microphone impedance head in a method similar to that used by Gibiat and Laloë. However, to obviate the need to know the complex wave number precisely, we use three loads without any resonances: a quasi-infinite impedance; an almost purely resistive impedance; and a flange [calibration loads (d) in Table II]. The resistive impedance is in our case a pipe so long that the reflected wave returns reduced in amplitude by 80 dB or more. For lower frequencies, with loss less than 80 dB, it suffices to deliver the signal in pulses of duration  $T$  with  $T < 2L/c$ , where  $L$  is the length of the pipe.

The three calibration loads ( $\infty$ ,  $Z'$ , and  $Z''$ ) are measured and yield the measurement vectors  $\mathbf{b}$ ,  $\mathbf{b}'$ , and  $\mathbf{b}''$ . The measurements are made and the output spectrum optimized (see Sec. VI) using either a theoretical matrix  $\mathbf{A}$  derived from Eq. (2) or one derived from a previous calibration on the same measurement head. We then have the three calibration equations

$$p\mathbf{A} \begin{bmatrix} 1 \\ 0 \end{bmatrix} = \mathbf{b}, \quad (4)$$

$$p'\mathbf{A} \begin{bmatrix} 1 \\ 1/\bar{Z}' \end{bmatrix} = \mathbf{b}', \quad (5)$$

$$p''\mathbf{A} \begin{bmatrix} 1 \\ 1/\bar{Z}'' \end{bmatrix} = \mathbf{b}'', \quad (6)$$

where the bar represents a reduced impedance ( $\bar{Z} \equiv Z/Z_0$ ) and  $p$ ,  $p'$ , and  $p''$  are the pressures at the reference plane during measurement of each of the three calibration loads. Dividing each subsequent row in Eq. (4) by the first row yields the first column of  $\mathbf{A}$ ,

$$A_{j1} = A_{11}b_j/b_1, \quad (7)$$

in terms of  $A_{11}$ .  $A_{11}$  can be given any value without affecting impedance measurements; it is usually set equal to

$\cosh(ikx_1)$  (equivalent to assuming the first microphone has unity gain and that the measurement duct is cylindrical).

Taking pairs of rows from Eq. (5), we may eliminate  $p'$  and obtain linear equations in the unknowns  $A_{j2}$ . For example, rows 1 and 2 combine to give  $b'_2(A_{11}+A_{12}/\bar{Z}') = b'_1(A_{21}+A_{22}/\bar{Z}')$ . The elements  $A_{j2}$  are determined by eliminating the pressure ( $p'$  or  $p''$ ) from each pair of rows in Eqs. (5) and (6) and solving the resulting system. Note that for all  $n > 2$  the system is overdetermined (in the algebraic, noise-free sense) and for  $n=2$  is algebraically equivalent to the TMTTC technique of Gibiat and Laloë.

So, e.g., for a head with two microphones, calibrated with three known loads,

$$\begin{bmatrix} b'_2/\bar{Z}' & -b'_1/\bar{Z}' \\ b''_2/\bar{Z}'' & -b''_1/\bar{Z}'' \end{bmatrix} \begin{bmatrix} A_{12} \\ A_{22} \end{bmatrix} = \begin{bmatrix} b'_1A_{21} - b'_2A_{11} \\ b''_1A_{21} - b''_2A_{11} \end{bmatrix}. \quad (8)$$

The above-outlined calibration technique assumes very little about the geometry of the impedance head and the characteristics of the transducers. If the calibration is complete, then wall losses within the impedance head do not need to be taken into account explicitly. In the multiple microphone technique with cylindrical waveguide and microphones attached at known distances from the reference plane, the calibration parameters may be recast in a more instructive form. If each microphone has an admittance of  $y_j/Z_0$ , then the pressure and upstream flow at microphone  $j$  are related to those at microphone  $j-1$  according to

$$\begin{bmatrix} p_j \\ Z_0 U_j^+ \end{bmatrix} = \begin{bmatrix} 1 & 0 \\ -y_j & 1 \end{bmatrix} \mathbf{T} \begin{bmatrix} p_{j-1} \\ Z_0 U_{j-1}^+ \end{bmatrix}, \quad (9a)$$

where  $\mathbf{T}$  is the transfer matrix for a cylindrical pipe

$$\mathbf{T} = \begin{bmatrix} \cosh(ikd_j) & \sinh(ikd_j) \\ \sinh(ikd_j) & \cosh(ikd_j) \end{bmatrix} \quad (9b)$$

and  $d_j = x_j - x_{j-1}$ . For  $j=1$ ,  $p_{j-1}$  and  $U_{j-1}^+$  are the pressure and flow at the reference plane and  $d_1 = x_1$ . The microphone signals are equal to  $\kappa_j p_j$ , where  $\kappa_j$  is the gain of microphone  $j$ . Taking Eq. (9) and a calibrated matrix  $\mathbf{A}$ , one can determine  $k$ ,  $\kappa_j$  for  $j=1, \dots, n$  and  $y_j$  for  $j=1, \dots, n-1$  ( $y_n$ , the dimensionless admittance of the microphone closest to the source, cannot be determined). For a measurement setup with a combination of pressure and flow transducers, or all flow transducers, the calibration proceeds in much the same way and an equation similar to Eq. (9) can be constructed.

Sometimes a third calibration is unnecessary or impracticable. In these cases one may precalculate the complex wave number  $k$ , using a theory that accounts for viscothermal losses within the waveguide. For a given impedance head, a single set of three calibrations can determine the degree of confidence one may take in this assumption, and the errors involved in making it. The remaining elements of  $\mathbf{A}$  are then found from Eqs. (4) and (5) as described.

If one were confident in making further assumptions about the impedance head, then a single calibration may be used to determine either the microphone gains or admittances. For example, one might assume that  $y_j=0$  for  $j$

$=1, \dots, n-1$  (a reasonable assumption for small microphones coupled closely to a large waveguide). Then the matrix elements  $A_{j1}$  would be found from a measurement of the quasi-infinite impedance load [Eq. (7)] and the elements  $A_{j2}$  are given by

$$A_{j2} = A_{j1} \tanh(ikx_j). \quad (10)$$

Otherwise, we may decide to assume that  $\kappa_j=1$  for all  $j$  and determine the microphone admittances from the quasi-infinite impedance calibration using Eq. (9).

### C. Choice of calibration loads

The TMTTC technique works well for small frequency ranges but depends critically on the theory used to account for wall losses. Larger frequency ranges can be covered by using several microphone spacings and calibration tubes. By using the general technique presented earlier, where the signals from two or more microphones are processed simultaneously, a wide frequency range can be covered without measuring piecewise. The three resonant-free calibration loads used here are sufficient to determine the calibration parameters over the entire frequency range, although the impedance for the flange calibration must be derived from theory. For an impedance head with cylindrical waveguide, and nearly ideal microphones at known distances from the reference plane, one or more of the calibration loads may be omitted. Thus calibrating with the quasi-infinite impedance alone may be sufficient for many applications. If another calibration is required and a resistive impedance load is not available, one or more closed tubes of different length may be used instead. Then  $\bar{Z}'$  in Eq. (5) is the reduced impedance of the closed tube and several such equations should be solved simultaneously if several closed tubes are used (to choose resonant tube lengths see Gibiat and Laloë<sup>13</sup>).

## V. ERRORS

### A. Inadequate spectral resolution

Large resonances are usually present in any duct system used to measure acoustic impedance. As discussed by Bodén and Åbom<sup>9</sup> in the context of the two-microphone method, the pressure spectrum at each microphone varies periodically with frequency, due both to changes in the standing wave pattern in the duct as frequency is varied, and to resonances of the total duct system. When this pressure spectrum is estimated with a frequency resolution  $\Delta f$ , the period of any variation in the spectrum must be large compared to  $\Delta f$  in order to avoid errors associated with resonances in the head and impedance system. For this reason, the microphones should be positioned as close as possible to the impedance to be measured, and the duct length should be kept small. Some acoustic damping between the loudspeaker and the transducers may be used to reduce the amplitude of these duct resonances.

### B. Nonlinear transducer responses

Microphone and loudspeaker distortion can both produce errors in a measured impedance. In methods where the

impedance is calculated solely from the signals of two or more transducers obtained simultaneously, a distorting loudspeaker will not affect the measurement, as the distortion is present in each transducer signal and is canceled out. In methods using a single transducer and attenuator, loudspeaker distortion will only affect the measurement if it changes with the load (possible at impedance extrema). Distortion in the transducers will produce errors in the measured impedance. Microphone distortion is always present but is reduced at lower pressures, and the excitation signal may be adjusted to achieve a compromise between random noise and distortion. In this study, the compromise between these two effects was made during calibration on the quasi-infinite impedance by adjusting the output signal level to give microphone signal ratios with minimal contamination from random noise or distortion (as measured by the deviation of the signal from a smooth curve on a small frequency scale).

### C. Diameter mismatch at the reference plane

At any bore discontinuity, nonpropagating modes are evoked. Automotive mufflers usually have several such discontinuities. Most woodwind instruments have such discontinuities (for example at tone holes), but provided they are located a sufficient distance from the input, they do not influence the measurement of the plane-wave impedance. If, however, a discontinuity is present at the reference plane, the measured impedance will not be the plane-wave impedance of the object but some combination of the elements of the generalized impedance matrix described by Pagneux *et al.*<sup>26</sup>

The difference between the measured impedance and the “true” plane-wave impedance may be determined by multimodal theory and expressed as an error term. Alternatively, if an impedance head is calibrated on pipes with entry diameter equal to the entry diameter of the object under study, higher modes evoked at the reference plane are automatically taken into account.<sup>13</sup> In practice this approach requires many sets of calibration pipes, and it is often easier to apply one of the following corrections.

Van Walstijn *et al.*<sup>15</sup> discuss the effect of a duct discontinuity in the context of the two-microphone technique, but the results are applicable to any system where the transducers are a sufficient distance from the reference plane to measure only plane waves. They derive an expression for a suitable correction term, providing that all higher modes excited at the reference plane are evanescent and do not couple to any higher modes in other parts of the object.

If a volume flow source is used [see method (a) in Table I], the attenuator output and microphone will be located at, or very close to, the reference plane. Brass and Locke<sup>27</sup> and Fletcher *et al.*<sup>28</sup> have derived suitable correction terms for this situation.

An impedance determined by applying the above-mentioned corrections will usually be less accurate than one measured with a matching impedance head, as turbulent losses are not taken into account in the multimodal model.

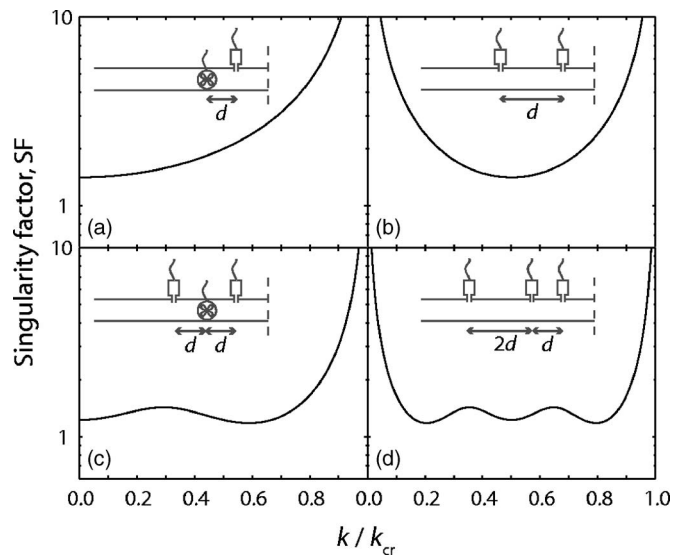


FIG. 2. Singularity factors plotted from  $k=0$  to the first singularity for several impedance heads (shown schematically in inset). The heads comprise (a) a microphone and anemometer, (b) two microphones, (c) two microphones and an anemometer, and (d) three microphones. For (a) and (c)  $k_{cr}d = \pi/2$  while for (b) and (d)  $k_{cr}d = \pi$ .

### D. Random noise (acoustical or electrical)

Each transducer signal is contaminated by random noise. Whether this is of acoustical or electrical origin is usually unimportant. This noise often has an overall  $1/f^n$  dependence, where  $0 < n < 1$  and the quality of measurements may be improved by increasing the power in the lower frequencies.

### E. The “singularity factor”

The sensitivity of any impedance head to errors in the input quantities varies over frequency. In the two-microphone method, for example, the head becomes “singular” when the microphone spacing is an integral multiple of  $\lambda/2$  and in this vicinity large errors in impedance result from small measurement errors. Conversely, for a microphone spacing of  $\lambda/4$ , the head is least sensitive to errors in the measured quantities. This effect is conveniently represented by the function SF (for singularity factor), defined by Jang and Ih,<sup>23</sup> their Eq. (16), and derived from the singular value decomposition of the matrix  $\mathbf{A}$ . (Jang and Ih are primarily interested in reflection coefficients, and their matrix  $\mathbf{A}$  relates the incident and reflected wave forms to the measured pressures. Their expression for SF remains valid when our modified matrix  $\mathbf{A}$  is used.) The singularity factor is useful to compare different impedance heads according to their sensitivity to measurement errors. SF is plotted for four systems in Fig. 2. Here attenuation is neglected and ideal transducers are assumed. The head in (a) utilizes a flow transducer and a microphone coupled to the duct at different positions. SF for this setup is smallest at low wave number and has a singularity when the distance between the transducers is equal to a quarter wavelength. In order to reduce error, the transducers should be as close as practicable to each other. However they are often separated by some distance, and the effect of this on the error in  $Z$  should not be neglected. Also, if the trans-

ducers deviate at all from ideality, they may be considered as ideal transducers separated by a certain effective “distance” (which may be complex and frequency dependent),<sup>25</sup> and two such transducers may exhibit behavior as depicted in Fig. 2(a) even if physically located at the same position.

In Figs. 2(b) and 2(d) SF is shown for heads comprising two and three microphones, respectively. These functions are singular at  $k=0$  and when the smallest microphone separation is equal to  $\lambda/2$ . Addition of the third microphone reduces SF over the entire frequency range and widens the range over which the method may be used. In Fig. 2(c) SF is shown for two microphones and a flow transducer; not surprisingly the function is lower than that for either Fig. 2(a) or 2(b) in isolation.

## F. Calculating the error in $Z$

Following Jang and Ih,<sup>23</sup> we may write the measured signals  $\tilde{\mathbf{b}}$  as the sum of the (hypothetical) real values,  $\mathbf{b}$ , and the measurement errors  $\mathbf{m}$ :

$$\tilde{\mathbf{b}} = \mathbf{b} + \mathbf{m}. \quad (11)$$

The errors in  $\mathbf{x}$  may then be written in terms of the measurement errors:

$$\tilde{\mathbf{x}} - \mathbf{x} = \mathbf{A}^+ \mathbf{m}, \quad (12)$$

where  $\mathbf{A}^+$  is the generalized (Moore-Penrose) inverse of  $\mathbf{A}$ .

If we right-multiply the error in  $\mathbf{x}$  by its complex conjugate transpose (denoted here by a superscript  $H$ ), the expectation value of the resulting matrix is given by

$$\begin{aligned} E[(\tilde{\mathbf{x}} - \mathbf{x})(\tilde{\mathbf{x}} - \mathbf{x})^H] &= E[(\mathbf{A}^+ \mathbf{m})(\mathbf{A}^+ \mathbf{m})^H] \\ &= E[\mathbf{A}^+ \mathbf{m} \mathbf{m}^H (\mathbf{A}^+)^H] = \mathbf{A}^+ \mathbf{V} (\mathbf{A}^+)^H, \end{aligned} \quad (13)$$

where  $\mathbf{V} = E[\mathbf{m} \mathbf{m}^H]$  is the covariance matrix. If each transducer signal is contaminated by uncorrelated noise of variance  $\sigma_j^2$ , where  $\sigma_j$  can in general be a function of frequency, then  $\mathbf{V}$  is a diagonal matrix with the  $\sigma_j^2$ s on the diagonal. The errors in  $p$  and  $U$ ,  $\Delta p$  and  $\Delta U$  are given by the diagonal elements of the matrix in Eq. (13):

$$|\Delta p|^2 = [\mathbf{A}^+ \mathbf{V} (\mathbf{A}^+)^H]_{11}, \quad (14)$$

$$|Z_0 \Delta U|^2 = [\mathbf{A}^+ \mathbf{V} (\mathbf{A}^+)^H]_{22} \quad (15)$$

and the error  $\Delta Z$  in the impedance  $Z$  is obtained by propagation of errors:

$$\frac{\Delta Z}{Z} = \sqrt{\left| \frac{\Delta p}{p} \right|^2 + \left| \frac{\Delta U}{U} \right|^2}. \quad (16)$$

The Pythagorean sum used in Eq. (16) is only strictly correct if the errors in  $p$  and  $U$  are independent. While this is not true in general, the equation will be approximately correct at impedance maxima and minima, where either  $|\Delta p/p| \gg |\Delta U/U|$  or  $|\Delta U/U| \gg |\Delta p/p|$ . At intermediate values of impedance, where  $|\Delta p/p| \approx |\Delta U/U|$ , Eq. (16) will overestimate the error. Since in this work we are mostly interested in impedance maxima and minima, use of Eq. (16) to estimate

the error will lead only to a more conservative redistribution of power.

The variance of the measurement errors may be estimated from experiment or simply assumed equal for each microphone, with possibly an  $f^{-0.5}$  dependence if the noise is of mostly acoustical origin. In this study the sound source was excited with repeated cycles of a periodic signal (see Sec. VI) and the microphone signals were synchronously acquired in blocks corresponding to one cycle of the excitation signal. Spectra were computed for each block and averaged to reduce noise. The standard deviation in these spectra was used to fit  $\sigma_j$  for each microphone as an exponential function of frequency. The  $\sigma_j$ s thus obtained were used to calculate the covariance matrix and the error in  $Z$  [Eqs. (14)–(16)].

## VI. OPTIMIZATION OF THE OUTPUT SIGNAL

To measure an impedance spectrum, an output signal covering all frequencies in the range is required. Some authors use a swept-sinusoid<sup>2</sup> as the output signal. However, this takes much longer than using a signal with all of the frequency components present, such as white noise or chirps. In the present work, a signal is generated as a sum of components of all sampled frequencies. This signal is applied to the loudspeaker and the impedance and error are calculated.

Initially, the wave is synthesized numerically from components of equal amplitude. To improve the signal-to-noise ratio, the relative phases are adjusted so as to reduce the ratio of the maximum of the sum of sinusoids to the amplitude of each sinusoid, as described by Smith.<sup>29</sup> A wave with a flat power spectrum at the computer does not result in the acoustical wave produced at the reference plane having a flat spectrum, however, because the amplifiers, loudspeaker, and connecting conduit all have frequency-dependent responses. These responses could be removed by calculating the power function and multiplying the output spectrum by its inverse (such an approach is used by Wolfe *et al.*<sup>6</sup>). A flat acoustical spectrum does not, however, produce a flat noise response, because a given head has greater sensitivity to noise at some frequencies than at others. This can be compensated for by multiplying the output spectrum by the correction factor

$$C_1(f) = \frac{\Delta Z}{Z^w} \quad (17)$$

(where  $w$  is a weighting factor that may be varied to give preference to impedance maxima or minima) and using the resulting wave form in a second impedance measurement. If there are significant nonlinearities in the loudspeaker system, this procedure may be repeated until  $C_1(f)$  is tolerably flat, but this is usually unnecessary.

## VII. MATERIALS AND METHODS

### A. The impedance spectrometer

For the experiments described in this paper the impedance spectrometer is configured as shown in Fig. 3. The signal is synthesized on a computer (Macintosh G4) and output via a nominal 24 bit DAC (MOTU 828) to a power amplifier and midrange speaker. A truncated cone helps match the

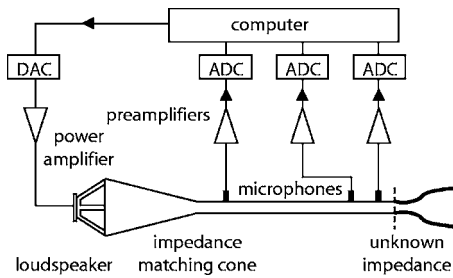


FIG. 3. The experimental setup. Calibration used two or three resonant-free calibration loads [see calibration loads (d) in Table II].

speaker to the measurement head. The impedance spectra are measured between 120 Hz and 4 kHz (a range that encompasses the fundamental frequency of all of the notes of many wind instruments, such as the clarinet and flute, and includes their cutoff frequency). It is easy to extend the frequency range of this technique to other instruments, e.g., the didjeridu.<sup>30</sup>

A brass measurement head was used with an inner diameter of 15.0 mm and with a 6 mm wall thickness. The brass construction and relatively massive design serve to lessen mechanical conduction of sound and reduce any temperature fluctuations as the head is handled during an experiment.

Three 1/4-in. condenser microphones (Brüel & Kjær 4944 A) are mounted in the impedance head, perpendicular to the cylindrical axis. A 1 mm hole couples each microphone to the waveguide. The compliance of these microphones (equivalent to an air volume of 0.25 mm<sup>3</sup> at 250 Hz) is negligible compared to that of the volume of air between the microphone and coupling hole, which together with the mass of air in the coupling hole forms a Helmholtz resonator with a natural frequency of 6.8 kHz. The coupling hole should be small enough so that the pressure wave is sampled over a distance small compared to its wavelength, and (for measurements using fewer than three calibrations) so that the impedance head is cylindrical, to a good approximation. On the other hand, it should be large enough so that the Helmholtz frequency of the microphone and coupling is much higher than the highest measured frequency. The chosen size of 1 mm represents a compromise between these competing considerations. The three microphones are mounted at 10, 50, and 250 mm from the reference plane. With the microphones positioned thus, a singularity occurs at  $\lambda=80$  mm, which for  $c=345$  m s<sup>-1</sup> corresponds to a frequency of 4.3 kHz (outside the frequency range of interest).

The signals from each microphone are preamplified and adjusted for calibrated gain by a Brüel & Kjær Nexus conditioning amplifier (2693-0S4) and digitized and recorded by the MOTU interface and the AUDIODESK software package. Wave forms are sampled at 44.1 kHz throughout and the output wave form is synthesized at 2<sup>14</sup> points (giving a frequency resolution of 2.7 Hz). To improve the signal-to-noise ratio the output is cycled repeatedly (100 cycles are typical, resulting in a total measurement time of 37 s) and the recorded signals are averaged. Fourier transforms are performed on the averaged data using the built-in functions in MATLAB.

## B. Calibration loads

The calibration loads (d) in Table II were used—a quasi-infinite impedance (brass plate), an almost purely resistive impedance (very long pipe), and a quasi-infinite flange.

As pointed out by Dalmont,<sup>25</sup> in most applications it is sufficient to assume that the admittance of a rigid wall is equal to zero (infinite impedance). Dalmont gives  $Z_0 Y_{\text{rigid}} = 9.6 \times 10^{-6} \sqrt{f}(1+i)$  for the reduced admittance of a rigid wall at 20 °C. For a tube of radius 10 mm at 100 Hz, the imaginary part of this admittance corresponds to a length correction of 0.05 mm and the real part to viscothermal dissipation on a length of 3 mm.

The almost purely resistive impedance is a straight PVC pipe of length 97 m and 15 mm internal diameter. The pipe is capped at its far end and filled with a small length (approximately 100 mm) of acoustically absorbing wool. If one assumes a fully reflective termination, i.e., neglecting the low reflection termination, at 120 Hz the reflected wave returns with a loss of at least 76 dB.<sup>24</sup> The actual loss at 120 Hz will be greater than this lower-bound due to absorption by the acoustic wool. The loss will also increase at higher frequencies due to viscothermal effects. Thus if there were equal power at each of the approximately 1400 frequencies, each reflected component would lie below the effective resolution of the ADC (~105 dB).

The quasi-infinite flange is a square perspex plate of side 600 mm in the center of which is a hole for mounting on the measurement head (for the end effect of a square flange see Dalmont *et al.*<sup>31</sup>). Over the frequency range of interest the impedance of a flange is lower than that of the resistive impedance load and so these three loads give complementary information. Preliminary experiments have shown that the inclusion of the third load changes the calibration very little, thereby justifying the assumptions made about propagation in the waveguide, and so it was omitted for most measurements.

## VIII. RESULTS AND DISCUSSION

### A. Effect of optimizing the output signal

As discussed earlier, equal distribution of energy among frequencies does not result in equal distribution of errors in the measurements, and the size of the largest error can be substantially reduced by adjusting the output spectrum for particular circumstances and loads.

Figure 4 shows the magnitude of and (absolute) fractional error in the measured impedance for three sequential impedance measurements. The error was calculated using Eqs. (14)–(16). In Fig. 4(a), the impedance  $Z$  of the resistive impedance load is measured with a nonideal source. The measured impedance spectrum is not completely flat since this measurement was performed before calibration. The error function  $\Delta Z/Z$  in Fig. 4(a) has broad features corresponding primarily to loudspeaker and conduit resonances. The output spectrum is multiplied by the error function in Fig. 4(a) and used to measure an open pipe [Fig. 4(b)]. The output spectrum is again multiplied by the error function and the pipe is measured a second time. The error in the resulting measurement [Fig. 4(c)] is uniformly distributed over fre-

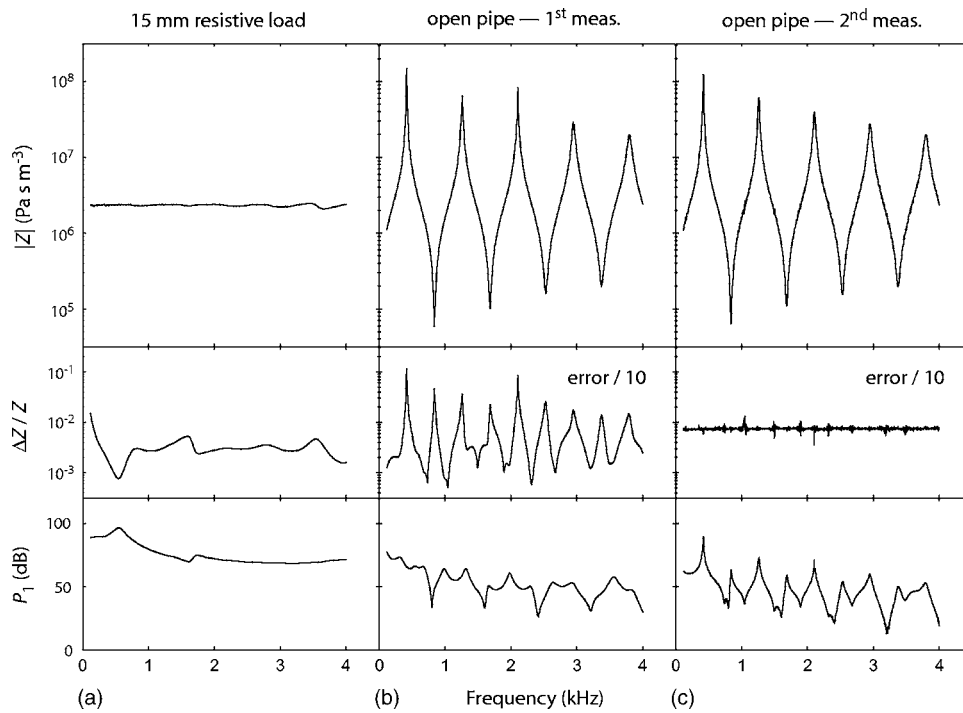


FIG. 4. Optimizing the output signal for measurements on 15 mm pipes. Impedance magnitude (upper panel) and fractional error (middle panel) are shown for (a) the 15 mm resistive impedance load measured with a non-ideal source and for an open pipe of length 200 mm measured with a deliberately very low signal (b) before and (c) after optimization. The error spectra in (b) and (c) have been scaled for comparison with (a). Also shown for each measurement is the sound pressure in dB re 20  $\mu$ Pa (lower panel) as measured by the microphone nearest to the reference plane.

quency. The errors shown in Figs. 4(b) and 4(c) have been divided by a factor of 10 (the signal amplitude was deliberately kept smaller than optimum to increase the apparent errors).

It is worth noting that in the uncorrected measurement (b) very high or very low impedances are measured with a greater error than are impedances close to  $Z_0$ . This is unfortunate in the case of musical instruments where we are particularly interested in impedance maxima and/or minima. On subsequent iterations, more power is put into these frequencies and the error is thereby reduced. As can be seen in Fig. 4(c), the error increases for impedances close to  $Z_0$  (the error is also more apparent here since the slope of the curve is not as steep as at impedance extrema). However, the maximum error over the entire spectrum is reduced by a factor of approximately 10 through this optimization procedure.

Also shown in Fig. 4 is the sound pressure spectrum measured by the microphone closest to the reference plane for each measurement. This is relatively uniform over frequency for the measurement of the resistive impedance and has minima corresponding to nodes of the standing wave for measurements of the 200 mm closed pipe.

The choice of the exponent  $w$  in  $C_1(f)$  [Eq. (17)] determines which part of the spectrum will be measured with the greatest precision. For  $w=1$ , the fractional error will be constant for all impedances. For  $w>1$ , the impedance minima will be determined with greater precision, and for  $w<1$  the impedance maxima will be given preference. The case where  $w>1$  is particularly useful for measuring the impedance of instruments in the flute family, which play near impedance minima, whereas  $w<1$  is useful for reed and lip valve instruments such as the clarinet which play near impedance maxima.

In some cases (such as when measuring calibration loads) it is not desirable to use the function  $C_1(f)$  to modify

the output spectrum, but we may still like to compensate for the system responses and the singularity factor of the head. In these cases, we modify the output spectrum to ensure that the acoustic energy density at the reference plane is the same as it would be during a (hypothetical) measurement of  $Z_0$  with  $\Delta Z/Z=K$  where  $K$  is independent of frequency. The acoustic energy density at the reference plane during a measurement of an impedance  $Z$  is proportional to  $\epsilon=(|p|^2+|Z_0U|^2)/2$ . For a measurement of  $Z_0$ ,

$$\epsilon_0=|Z_0U|^2=\frac{|\Delta p|^2+|Z_0\Delta U|^2}{K^2}, \quad (18)$$

where Eq. (16) was used for  $K$  with the substitution  $p=Z_0U$ . The correction factor  $C_2(f)$  used to modify the output spectrum will be proportional to the square root of the energy ratio  $\epsilon_0/\epsilon$ . We use

$$C_2(f)=K\sqrt{\frac{\epsilon_0}{\epsilon}}=\sqrt{2}\sqrt{\frac{|\Delta p|^2+|Z_0\Delta U|^2}{|p|^2+|Z_0U|^2}}, \quad (19)$$

where the factor  $K$  has no effect on the output wave form (being independent of frequency) but is used to ensure that  $C_2(f)=\Delta Z/Z$  when  $Z=Z_0$ .

## B. Effect of calibration

Figure 5 illustrates the effects of calibrating with varying numbers of known calibration loads. Measured impedance spectra are shown for a closed 15 mm pipe, 200 mm long. To simulate the effect of using unmatched microphones, in Figs. 5(a) and 5(b) the signals from the second and third microphones were scaled by 1.2 and 0.8, respectively. The measured impedance spectrum before calibration (i.e., assuming unity gain for each microphone) is shown in Fig. 5(a), while in Fig. 5(b) the impedance was calculated

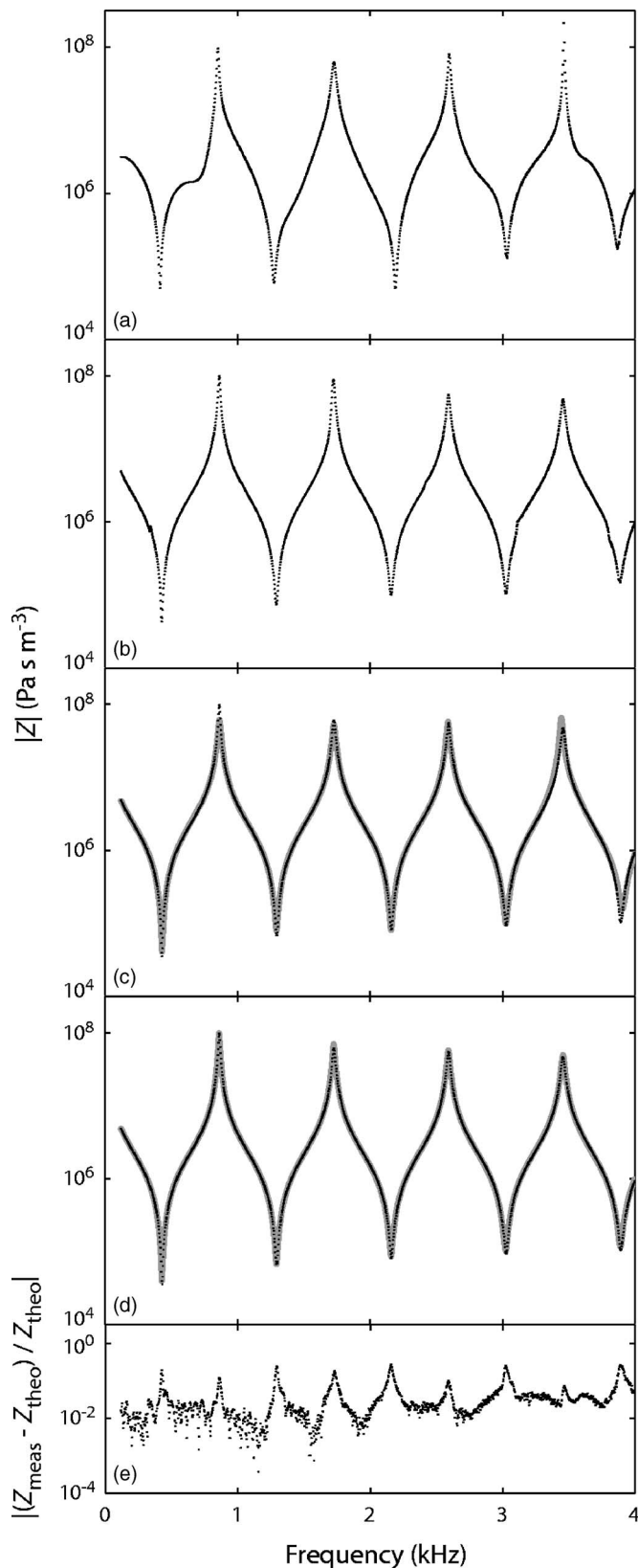


FIG. 5. The input impedance for a closed 15 mm pipe, 200 mm long. In (a) and (b) the signals from microphones 2 and 3 were multiplied by 1.2 and 0.8, respectively, to deliberately introduce errors. The impedance was measured before calibration (a) and after calibrating using one known load (b). In (c) the impedance is given for matched microphones before (grey, solid line) and after (black, dotted line) calibration with two known loads, and in (d) the calibrated measurement from (c) (black, dotted line) is compared with the theoretical impedance for an ideal tube (grey, solid line). The fractional difference between this theory and the measurement is shown in (e).

after calibrating on the quasi-infinite impedance load [using Eqs. (7) and (10)]. The precalibration measurement deviates significantly from the theoretical impedance, while calibrating with only one load (b) improves the accuracy significantly. In Fig. 5(c) the measured impedance spectrum using the matched microphone signals is shown before and after calibration with two known loads. While the two spectra are similar in many respects, the size and frequency of extrema (particularly maxima) are significantly different. For this measurement, adding the flange calibration made very little difference. The measurement made without using the two calibration loads shows similar features to those of the precise measurement over most of the range, but has noticeable errors in the magnitude of extrema (particularly maxima) and smaller errors in the frequencies at which they occur. In Fig. 5(d) the measurement on the 200 mm closed pipe using two calibration loads is compared with the theoretical impedance and the fractional difference between these two measurements is shown in Fig. 5(e). The peaks in this difference function at impedance extrema are likely due to slightly greater attenuation in the measured impedance than is predicted by the theory for viscothermal losses at walls that are ideally smooth.

### C. Conclusions and practical considerations for measurement

The combination of three microphones, three nonresonant calibrations, and spectral shaping can give precise measurements over a wide range of frequencies and impedance. It has the added advantage that no assumptions need be made about the microphone characteristics or about the exact geometry of the impedance head. Furthermore, there is no need to invoke a theoretical model for waveguide losses.

In many practical measurement situations, however, the reduced performance of a simpler combination might still be appropriate.

Thus two microphones, rather than three, would often be sufficient for a smaller frequency range (perhaps 2–3 octaves, depending upon the precision required).

In many practical cases, fewer than three nonresonant calibrations might be sufficient, albeit with some loss in performance. Thus if a well-defined cylindrical impedance head is used, and if the perturbations of the cylinder by the microphones are sufficiently small, it is possible to remove one calibration (this is a consequence of the good theoretical model available for a cylindrical waveguide). It is also possible to remove one calibration if the characteristics of the microphones are already known with a high degree of precision.

The redistribution of power in the source function (spectral shaping) can improve the signal-to-noise ratio at extrema by a factor of 10 or more. Whether or not this feature is needed depends on the size of errors that may be tolerated in the measurements. Further, this feature would be less important if the unknown impedance has no strong resonances.

## ACKNOWLEDGMENTS

Technical assistance and advice was provided by John Tann. P.D. was supported by an Australian Postgraduate Award (Industry) jointly funded by the Australian Research Council, the Powerhouse Museum, and Terry McGee (flute-maker).

- <sup>1</sup>A. H. Benade and M. I. Ibsi, "Survey of impedance methods and a new piezo-disk-driven impedance head for air columns," *J. Acoust. Soc. Am.* **81**, 1152–1167 (1987).
- <sup>2</sup>J.-P. Dalmont, "Acoustic impedance measurement. I. A review," *J. Sound Vib.* **243**, 427–439 (2001).
- <sup>3</sup>A. P. Watson and J. M. Bowsher, "Impulse measurements on brass musical instruments," *Acustica* **66**, 170–174 (1988).
- <sup>4</sup>J. J. Fredberg, M. E. B. Wohl, G. M. Glass, and H. L. Dorkin, "Airway area by acoustic reflections measured at the mouth," *J. Appl. Physiol.: Respir., Environ. Exercise Physiol.* **48**, 749–758 (1980).
- <sup>5</sup>R. Singh and M. Schary, "Acoustic impedance measurement using sine sweep excitation and known volume velocity technique," *J. Acoust. Soc. Am.* **64**, 995–1003 (1978).
- <sup>6</sup>J. Wolfe, J. Smith, J. Tann, and N. H. Fletcher, "Acoustic impedance spectra of classical and modern flutes," *J. Sound Vib.* **243**, 127–144 (2001).
- <sup>7</sup>A. M. Bruneau, "An acoustic impedance sensor with two reciprocal transducers," *J. Acoust. Soc. Am.* **81**, 1168–1178 (1987).
- <sup>8</sup>M. Åbom and H. Bodén, "Error analysis of two-microphone measurements in ducts with flow," *J. Acoust. Soc. Am.* **83**, 2429–2438 (1988).
- <sup>9</sup>H. Bodén and M. Åbom, "Influence of errors on the two-microphone method for measuring acoustic properties in ducts," *J. Acoust. Soc. Am.* **79**, 541–549 (1986).
- <sup>10</sup>J. Y. Chung and D. A. Blaser, "Transfer function method of measuring acoustic intensity in a duct system with flow," *J. Acoust. Soc. Am.* **68**, 1570–1577 (1980).
- <sup>11</sup>J. Y. Chung and D. A. Blaser, "Transfer function method of measuring in-duct acoustic properties. I. Theory," *J. Acoust. Soc. Am.* **68**, 907–913 (1980).
- <sup>12</sup>J. Y. Chung and D. A. Blaser, "Transfer function method of measuring in-duct acoustic properties. II. Experiment," *J. Acoust. Soc. Am.* **68**, 914–921 (1980).
- <sup>13</sup>V. Gibiat and F. Laloë, "Acoustical impedance measurements by the two-microphone-three-calibration (TMTC) method," *J. Acoust. Soc. Am.* **88**, 2533–2545 (1990).
- <sup>14</sup>A. F. Seybert and D. F. Ross, "Experimental determination of acoustic properties using a two-microphone random-excitation technique," *J. Acoust. Soc. Am.* **61**, 1362–1370 (1977).
- <sup>15</sup>M. van Walstijn, M. Campbell, J. Kemp, and D. Sharp, "Wideband measurement of the acoustic impedance of tubular objects," *Acust. Acta Acust.* **91**, 590–604 (2005).
- <sup>16</sup>J. Backus, "Input impedance curves for the reed woodwind instruments," *J. Acoust. Soc. Am.* **56**, 1266–1279 (1974).
- <sup>17</sup>J. Backus, "Input impedance curves for the brass instruments," *J. Acoust. Soc. Am.* **60**, 470–480 (1976).
- <sup>18</sup>R. Caussé, J. Kergomard, and X. Lurton, "Input impedance of brass musical instruments—Comparison between experiment and numerical models," *J. Acoust. Soc. Am.* **75**, 241–254 (1984).
- <sup>19</sup>F. J. M. van der Eerden, H.-E. de Bree, and H. Tijdeman, "Experiments with a new acoustic particle velocity sensor in an impedance tube," *Sens. Actuators, A* **A69**, 126–133 (1998).
- <sup>20</sup>S. Elliott, J. Bowsher, and P. Watkinson, "Input and transfer response of brass wind instruments," *J. Acoust. Soc. Am.* **72**, 1747–1760 (1982).
- <sup>21</sup>M. Kob and C. Neuschaefer-Rube, "A method for measurement of the vocal tract impedance at the mouth," *Med. Eng. Phys.* **24**, 467–471 (2002).
- <sup>22</sup>R. L. Pratt, S. J. Elliott, and J. M. Bowsher, "The measurement of the acoustic impedance of brass instruments," *Acustica* **38**, 236–246 (1977).
- <sup>23</sup>S.-H. Jang and J.-G. Ih, "On the multiple microphone method for measuring in-duct acoustic properties in the presence of mean flow," *J. Acoust. Soc. Am.* **103**, 1520–1526 (1998).
- <sup>24</sup>N. H. Fletcher and T. D. Rossing, *The Physics of Musical Instruments*, 2nd ed. (Springer, New York, 1998).
- <sup>25</sup>J.-P. Dalmont, "Acoustic impedance measurement. II. A new calibration method," *J. Sound Vib.* **243**, 441–459 (2001).
- <sup>26</sup>V. Pagneux, N. Amir, and J. Kergomard, "A study of wave propagation in varying cross-section waveguides by modal decomposition. I. Theory and validation," *J. Acoust. Soc. Am.* **100**, 2034–2048 (1996).
- <sup>27</sup>D. Brass and A. Locke, "The effect of the evanescent wave upon acoustic measurements in the human ear canal," *J. Acoust. Soc. Am.* **101**, 2164–2175 (1997).
- <sup>28</sup>N. H. Fletcher, J. Smith, A. Z. Tarnopolsky, and J. Wolfe, "Acoustic impedance measurements—Correction for probe geometry mismatch," *J. Acoust. Soc. Am.* **117**, 2889–2895 (2005).
- <sup>29</sup>J. R. Smith, "Phasing of harmonic components to optimize measured signal-to-noise ratios of transfer functions," *Meas. Sci. Technol.* **6**, 1343–1348 (1995).
- <sup>30</sup>J. Smith, G. Rey, P. Dickens, N. Fletcher, L. Hollenberg, and J. Wolfe, "Vocal tract resonances and the sound of the Australian didgeridu (yidaki). III. Determinants of playing quality," *J. Acoust. Soc. Am.* **121**, 547–558 (2007).
- <sup>31</sup>J.-P. Dalmont, C. J. Nederveen, and N. Joly, "Radiation impedance of tubes with different flanges: Numerical and experimental investigations," *J. Sound Vib.* **244**, 505–534 (2001).